SCIENTIFIC REPORTS

OPEN

SUBJECT AREAS:
BIOPHYSICS
BIOMEDICAL ENGINEERING
ION CHANNELS IN THE NERVOUS SYSTEM

Received
24 April 2014

Accepted
9 July 2014

Published
25 July 2014

Correspondence and requests for materials should be addressed to E.E. (entcheva@stonybrook.edu)

Channelrhodopsin2 Current During the Action Potential: "Optical AP Clamp" and Approximation

Emilia Entcheva & John C. Williams

Department of Biomedical Engineering, Stony Brook University, Stony Brook, USA.

The most widely used optogenetic tool, Channelrhodopsin2 (ChR2), is both light- and voltage-sensitive. A light-triggered action potential or light-driven perturbations of ongoing electrical activity provide instant voltage feedback, shaping ChR2 current. Therefore, depending on the cell type and the light pulse duration, the typically reported voltage-clamp-measured ChR2 current traces are often not a good surrogate for the ChR2 current during optically-triggered action potentials. We discuss two experimental methods to reveal ChR2 current during an action potential: an "optical AP clamp" and its approximation employing measured current-voltage curve for ChR2. The methods are applicable to voltage- and light-sensitive ion currents operating in excitable cells, e.g. cardiomyocytes or neurons.

This brief note concerns the underlying opsin currents during light-triggered action potentials in excitable cells and tissues in optogenetics experiments. The most widely used excitatory opsin, Channelrhodopsin2 (ChR2), is both light- and voltage-sensitive[1,2]. This implies that during an optically-triggered action potential, the ChR2 current will experience instant feedback from the ensuing change in membrane voltage. Many optogenetics studies[2–6] show *side-by-side independent records* of the light-triggered ChR2 current (in *voltage-clamp mode* using a constant voltage setting), $I_{ChR2(Vclamp)}$, and the light-triggered change in membrane voltage (action potential, AP) obtained in *current-clamp mode*. Occasionally, the AP record and $I_{ChR2(Vclamp)}$ are shown in a paired manner[5,6]. However, the actual ChR2 current during the displayed action potential, $I_{ChR2(AP)}$, is never measured nor reported in the literature. We stress here that $I_{ChR2(Vclamp)}$ and $I_{ChR2(AP)}$ can be very different, especially for longer light pulses and/or longer action potentials, as seen in cardiomyocytes, for example. This is illustrated in the simulated examples in Figure 1, using a computer model of ChR2(H134R)[7] inserted in a human ventricular cardiomyocyte model[8] and in a modified Hodgkin-Huxley model of squid giant axon[9]. The action potential provides instant feedback and shapes the ChR2 current through voltage according to our model[7,10] and our experimental data for $I_{ChR2(AP)}$ in cardiomyocytes[7].

The classic way to experimentally extract the contribution of a voltage-dependent current during an action potential is to apply an *action potential clamp (APclamp)*[11,12] in conjunction with specific pharmacological blocking agents. Typically, a pre-recorded action potential (obtained under current-clamp regime, $I_{total} = 0$) is used as voltage input to clamp the cell and two records are obtained – in the absence ("no drug") and in the presence ("drug") of a selective pharmacological blocker. The difference in total current between the two conditions is interpreted as the current of interest.

Light-sensitive ion channels add a twist to this approach. The "drug" condition can be easily captured by a record of total current in the dark, which yields a very selective blocking of the opsin contribution. However, the "no drug" record of a light- and voltage-sensitive ion channel is non-trivial. While the action of pharmacological blockers is slow (compared to the action potential kinetics) and steady-state records are appropriate, the response to a light pulse(s) is instantaneous and it elicits an important fast transient component in ChR2 that needs to be preserved in the current record. Hence, constant "light on" condition will not be equivalent to "no drug". Recently, we presented a modified version of the *APclamp* that uses precisely synchronized optical pulse(s) to extract $I_{ChR2(AP)}$ during optically-triggered *APs*[7] – an *"optical APclamp"* method explained in Figure 2.

Additionally, here we propose an alternative scaling method for extracting $I_{ChR2(AP)}$ that corrects the measured $I_{ChR2(Vclamp)}$ using an empirical current-voltage (I–V) curve, fed by voltage values from the measured optically-triggered *APs*. The idea is inspired by the relatively mild voltage dependence of ChR2 kinetics[7] and therefore ability to separate[7,13–15] its light-dependence (L) and its voltage-dependence (a measured I–V curve). We begin with a general expression for I_{ChR2} as a function of irradiance $E[t]$, transmembrane voltage $V[t]$, and time t:

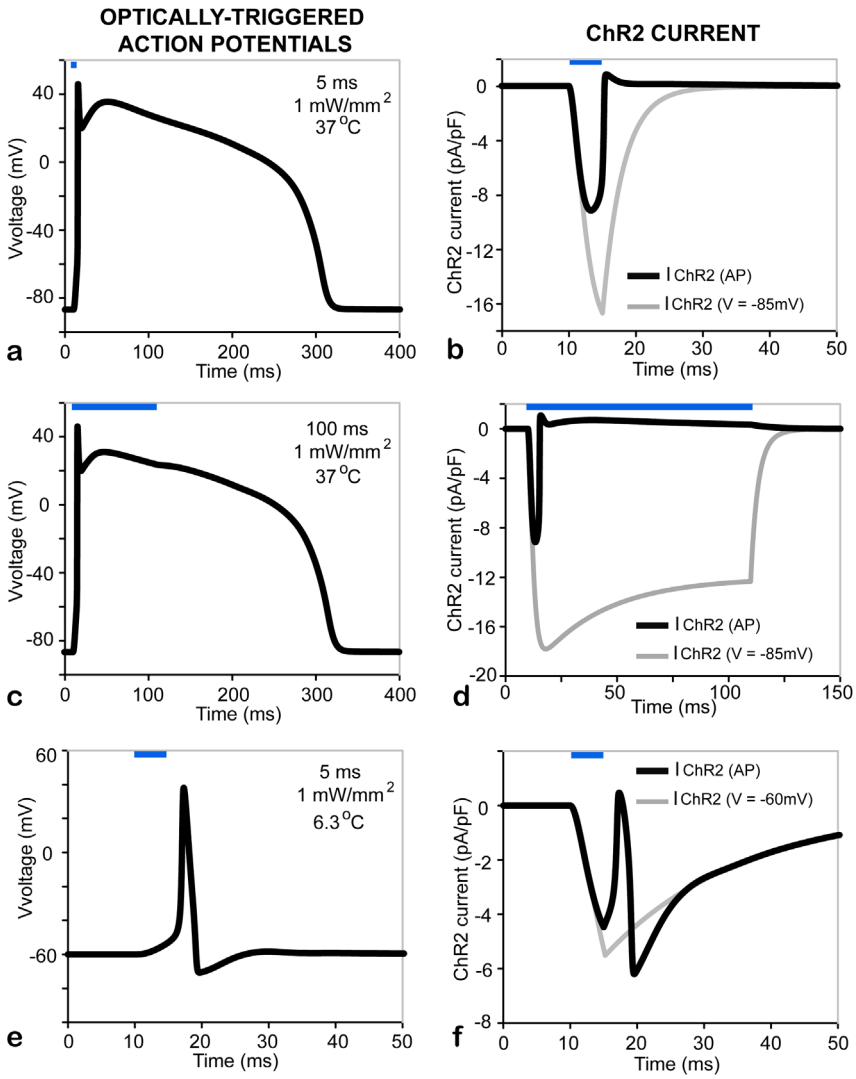

Figure 1 | ChR2 current during a light-triggered action potential is different from the ChR2 current in response to a constant voltage clamp using the same light pulse parameters (here 470 nm, 1 mW/mm²). (a–b). The response of a ventricular cardiomyocyte to a 5 ms light pulse. (c–d). The response of a ventricular cardiomyocyte to a 100 ms light pulse. (e–f). The response of a squid giant axon to a 5 ms light pulse. Panels a, c and e show the lighttriggered *APs*, while (b), (d) and (f) show $I_{ChR2(AP)}$. For comparison, $I_{IChR2(Vclamp)}$ in response to identical light pulses is overlaid (grey) in (b), (d) and (f) (Vclamp5285 mV or 260 mV). Cardiomyocyte simulations (a–d) were at 37°C, while the squid giant axon model (e–f) was run at 6.3°C. Blue bars indicate timing of light pulse application.

$$I_{ChR2}(E[t], V[t], t) = g_{ChR2} * G(V[t]) * L(E[t], V[t], t) \quad (1)$$

where *G(V[t])* is the voltage-dependent channel conductance (a non-linear inward rectifying function for ChR2), *L(E[t],V[t],t)* is the irradiance- and voltage-dependent kinetic response of the channel to light, and g_{ChR2} is a scaling factor for expression levels.

Then, for the ChR2 current during time-invariant clamp voltage, V_{clamp}, we obtain:

$$I_{ChR2(Vclamp)}(E[t], V_{clamp}, t) = g_{ChR2} * G(V_{clamp}) * L(E[t], V_{clamp}, t) \quad (2)$$

The mild voltage-dependence of the ChR2 kinetic parameters[7] permits the approximation of the kinetic response (in *L*) during dynamically changing voltage (e.g. action potentials) with the response during a voltage clamp, if in both cases an identical optical stimulation protocol is used, i.e. identical light pulse sequence is applied with the same irradiance, pulse morphology and duration, *E[t]*:

$$I_{ChR2(AP)}(E[t], V[t], t) \approx g_{ChR2} * G(V[t]) * L(E[t], V_{clamp}, t) \quad (3)$$

Therefore, from (2) and (3), a *scaler* function can be derived, which is purely voltage-dependent and independent of the light response (*L*) of the tissue:

$$\frac{I_{ChR2(AP)}(E[t], V[t], t)}{I_{ChR2(Vclamp)}(E[t], V_{clamp}, t)} \approx \frac{G(V[t])}{G(V_{clamp})} = scaler(V[t]) \quad (4)$$

In sum, any opsin current, $I_{ChR2(AP)}$, during optically-triggered dynamic voltage response, e.g. action potential(s), can be recovered using:

- a known I–V curve, *G(V[t])*
- measured light-triggered voltage response, *V[t]*, and
- measured $I_{ChR2(Vclamp)}[t]$ under voltage-clamp and identical light-pulsing protocol *E[t]*, used to obtain *V[t]*; $I_{ChR2(Vclamp)}[t]$ intrinsically carries information about the expression levels and light-dependent kinetics

$$I_{ChR2(AP)}(E[t], V[t], t) = scaler(V[t]) * I_{ChR2(Vclamp)}(E[t], V_{clamp}, t) \quad (5)$$

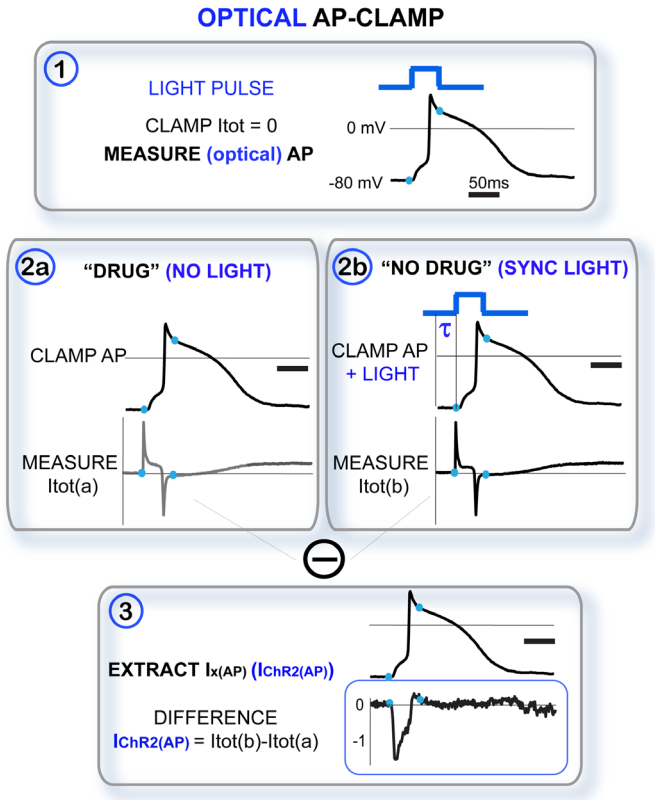

Figure 2 | The "optical APclamp": Experimental protocol to extract opsin current during an optically-triggered action potential. The schematic illustrates the three steps in a classical *APclamp* (in black) and the added elements to achieve an "*optical APclamp*" (in blue). Importantly, in step **2b**, identical light pulse(s) to the one(s) used in step **1** must be delivered synchronously (lag time **τ**) with the action potential clamp. The traces are used for illustration only but they are actual recordings from ChR2-expressing adult guinea pig cardiomyocytes, as shown in[7].

Step-by-step graphical illustration of this scaling method is shown in Figure 3, including derivation of the *scaler* function and application to model data from Figure 1. Furthermore, in Figure 3i, we apply this method to an example of published neuroscience data[6], using ChETA (a ChR2 mutant[16,17]). We computationally recover $I_{ChETA(AP)}$ in ChETA-expressing melanin-concentrating hormone (MCH) neurons, based on the published AP and $I_{ChETA(Vclamp)}$ records, and assuming similar rectification function as for ChR2(H134R), as implied in[16,17]. The predicted current $I_{ChETA(AP)}$ is substantially smaller and with different (biphasic) morphology than the $I_{ChETA(Vclamp)}$; this may explain the lack of secondary spikes compared to equivalent electrical current injection[6].

Errors in the proposed approximation approach come from: 1) uncertainties in the ChR2 I–V curve for the particular cell; and 2) from ignored voltage-dependence of the kinetic parameters of the light response (L), i.e. assumption (3). Errors of the first kind may occur primarily if the opsin (I–V) response varies significantly depending on the cell environment and the I–V curve was obtained in a different cell type than the one in which voltage is measured; importantly however, other conditions of the experiment, e.g. irradiance and pulse protocols, are captured independently of the I–V curve, through $I_{ChR2(Vclamp)}$ in Eqn. (5). Errors of the second type are relatively small for ChR2/H134R as displayed in Figure 3. This method is applicable to any opsin with a well-characterized I–V curve, and the accuracy of approximating $I_{ChR2(AP)}$ is inversely related to the level of voltage-dependence in the opsin's kinetics (in the L-function). In ChR2 mutants with relatively voltage-independent kinetics such as ChETA (E123T)[16] and ET/TC (E123T/T159C)[17], the method will be highly accurate, with even smaller approximation errors when compared with H134R. The use of this technique with such opsins renders the approximation in Eqn. (3) very accurate, as the kinetics of ChETA and ET/TC are completely recovered by measuring the current under voltage clamp (through $I_{ChR2(Vclamp)}$), and the *scaler* fully corrects for the rectification-induced nonlinearity in voltage. Furthermore, with knowledge of an opsin's selective ionic permeability, this method provides an effective tool for determining an opsin's transient ionic flux during ongoing electrical activity and therefore its contribution to intracellular ionic concentrations. This is particularly important for those with greater permeability to Ca^{2+} such as CatCh (L123C)[18] or when trying to predict an opsin's effect on intracellular pH[19]. Similar to H134R discussed here, ChETA, ET/TC, and CatCh all retain the strong inward rectification displayed by wild-type ChR2[16–18], thus it is similarly necessary to perform either this approximation or the aforementioned optical AP clamp to recover the true ChR2 current ($I_{ChR2(AP)}$) during dynamically changing voltage.

We expect the accuracy of the approximation method to be somewhat reduced for more complex light-pulsing protocols when recovery from inactivation is engaged, as the latter depends on voltage[7]. To test the performance of the proposed approach for multi-pulse protocols, we analyzed optical pacing of cardiomyocytes at different frequencies: 1 Hz, 5 Hz and 20 Hz *in silico* (Figures 4 and 5). Human ventricular cardiomyocytes show full capture, i.e. 1 : 1 response, during 1 Hz optical pacing at 5 ms pulses, 1 mW/mm^2 (Figure 4a). Same pulse parameters induce 2 : 1 block at 5 Hz pacing, i.e. every other pulse triggers an action potential (Figure 4b), and result in a higher-level block (8 : 1) at a very fast, unphysiological pacing rate of 20 Hz (Figure 4c). In all cases, the voltage-clamp recorded current, $I_{ChR2(Vclamp)}$, shown in rows II of all panels, is a poor surrogate for the "true" $I_{ChR2(AP)}$, shown as a black trace in rows III, Figure 4a–c. In contrast, our approximation/scaling approach fully captures the morphology of the true $I_{ChR2(AP)}$ (red vs. black trace in rows III), and tracks it quantitatively even at high pacing rates, with instantaneous maximum errors mostly less than 1 pA/pF (rows IV in Figure 4a–c).

The contrast in performance between the $I_{ChR2(Vclamp)}$ and our approximation of the true $I_{ChR2(AP)}$ is further quantified in Figure 5a vs. 5b. The relative time-integrated errors (δ(n) as per Eqn. (7)) for the former are unacceptably high even at 1 Hz pacing, and are more than 20 times higher than those seen with the proposed approximation.

$$\varepsilon(n) = \left| \int_0^{t_{end}} \left| I_{ChR2(approx)}(n,t) \right| dt - \int_0^{t_{end}} \left| I_{ChR2(AP)}(n,t) \right| dt \right| \quad (6)$$

$$\delta(n) = \frac{\varepsilon(n)}{\int_0^{t_{end}} \left| I_{ChR2(AP)}(n,t) \right| dt} * 100,\% \quad (7)$$

where n is the number of delivered optical pulses, t_{end} is the time when the (n-th) pulse period ends, $I_{ChR2(approx)}$ represents either $I_{ChR2(Vclamp)}$ (Figure 5a) or the approximated/scaled $I_{ChR2(AP)}$ (Figure 5b), and $\varepsilon(n)$ is the cumulative time-integrated absolute error (in units of charge, nC/μF) for n pulses (Figure 5c).

We also show the time-integrated absolute error per pulse (also in nC/μF), $\varepsilon_{pulse}(n)$, in Figure 5d:

$$\varepsilon_{pulse}(n) = \left| \int_{t_n}^{t_{n+1}} \left| I_{ChR2(approx)}(t) \right| dt - \int_{t_n}^{t_{n+1}} \left| I_{ChR2(AP)}(t) \right| dt \right| \quad (8)$$

where t_n is the onset of the n-th pulse and t_{n+1} is the start time of the following pulse.

With lack of full capture at higher pacing rates, i.e. 2 : 1 response at 5 Hz and 8 : 1 response at 20 Hz, the errors per pulse vary accordingly (Figure 5d), changing with the membrane potential and the level of

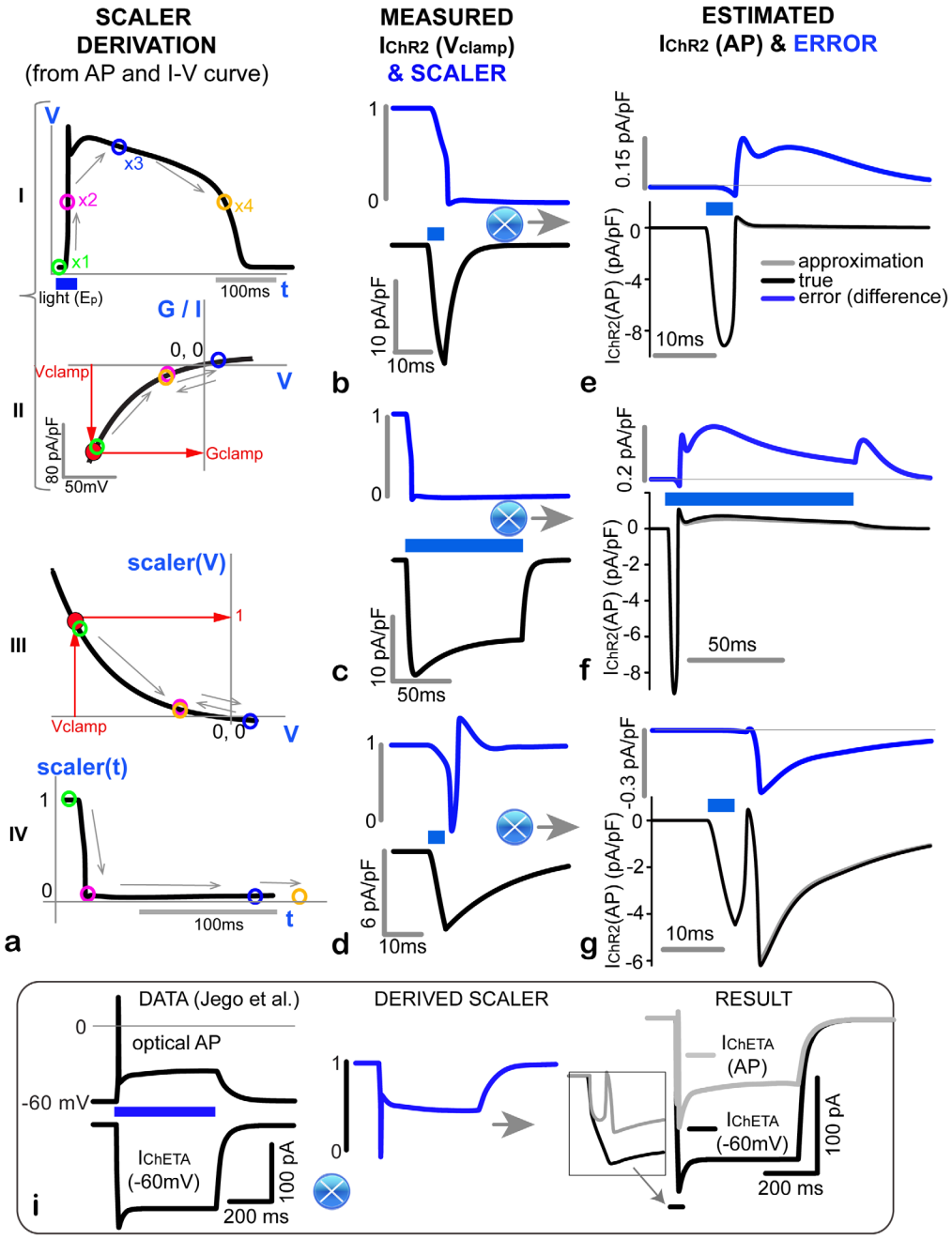

Figure 3 | Approximation to an "optical APclamp": Scaling $I_{ChR2(Vclamp)}$ by an experimental ChR2 I-V curve to obtain $I_{ChR2(AP)}$. (a). Derivation of a *scaler*, using an example light-triggered ventricular cell AP (a-I) and an empirical ChR2 I-V curve (a-II, here, the fit to the I-V curve had the form $G(V) = (10.64 - 14.64*exp(-V/42.77))$[7]). The position of four color-coded points (x1 to x4) from the *AP* is mapped onto the I–V curve and then onto the derived *scaler* as a function of voltage (a-III) and as a function of time (a-IV). Note the different time scales in a-I and a-IV. (b-g). Using the time-dependent *scaler* (middle column, (b–d), blue), derived for each of the three simulated cases from Figure 1, here we multiply the typically measured and reported $I_{ChR2(Vclamp)}$ (middle column, (b–d), black) to obtain an excellent approximation of the $I_{ChR2(AP)}$ (right column, (e–g)). Superimposed in (e–g) are the "true" (black) and approximated/scaled $I_{ChR2(AP)}$ (grey); the small error (difference between the two currents) is enhanced in blue for each case. The bottom panel (i) illustrates the application of the method to published data on ChETA-MCH neurons[6]; inset on the right shows the first 50 ms of measured $I_{ChETA(Vclamp)}$ and estimated $I_{ChETA(AP)}$.

ChR2 current engagement. Therefore, for a given number of pulses, the cumulative errors for very high pacing rates (20 Hz) can be lower than the errors seen for 1 Hz pacing, for example (Figure 5c). Nevertheless, in all cases, the approximation captures the morphology of $I_{ChR2(AP)}$ with small instantaneous errors (Figure 4).

When a light pulse triggers ChR2 response during an ongoing action potential, the contribution of this opsin-provided current strongly depends on the respective action potential shape, and hence on the voltage feedback provided by the cell. For example, in a ventricular cardiomyocyte, it is very difficult to alter an ongoing action potential if light stimulation is applied during the earlier AP phases, Figure 6, left, due to the strong inward rectification of ChR2 at the depolarized voltage levels maintained during the ventricular AP plateau. Furthermore, because of the rapid nonlinear voltage changes in the later repolarization AP phases, the observed $I_{ChR2(AP)}$ is very different in shape compared to $I_{ChR2(Vclamp)}$. At the same time, in

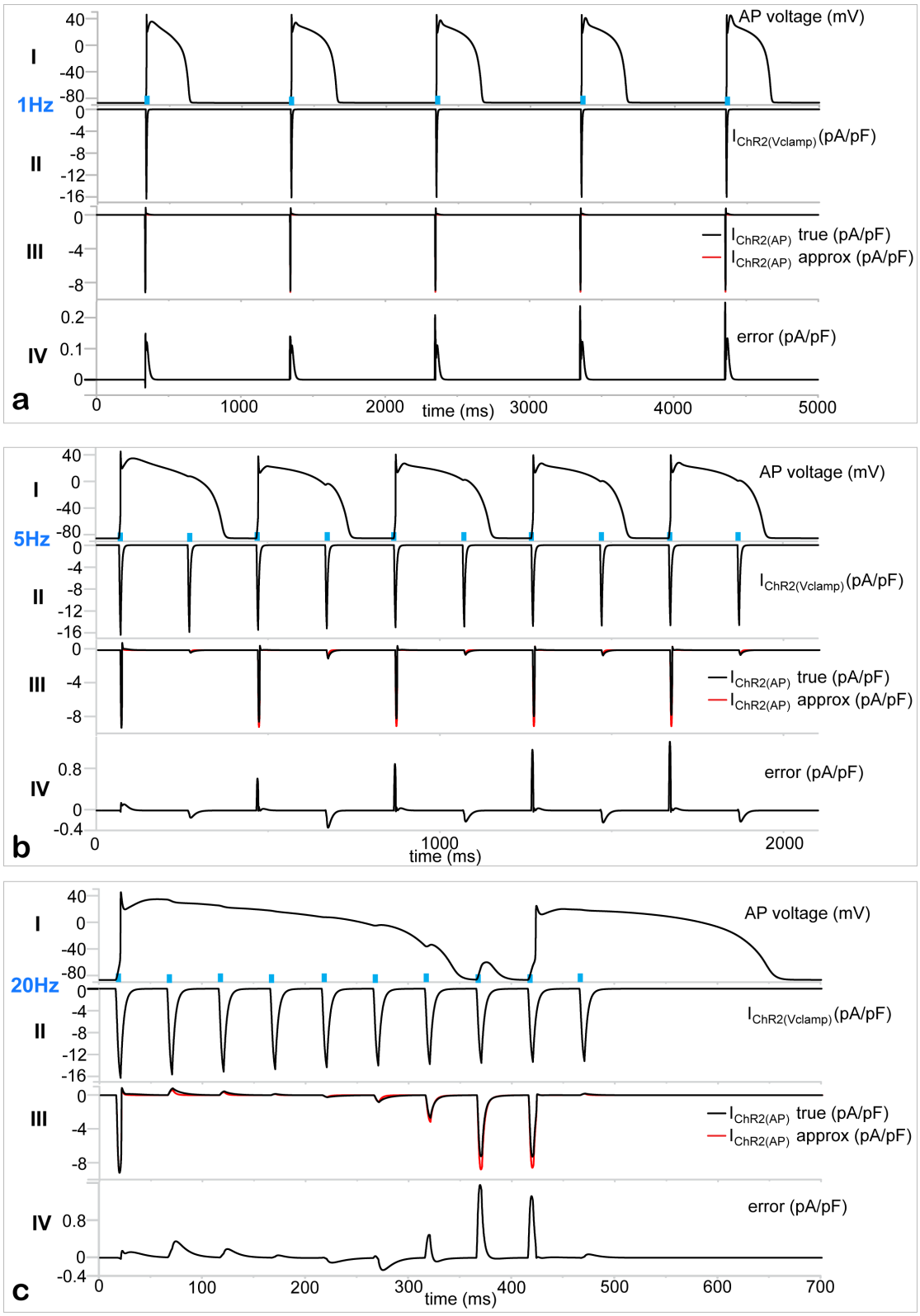

Figure 4 | Optical pacing of cardiomyocytes at various frequencies and the underlying $I_{ChR2(AP)}$ – example traces and approximation errors. Human ventricular cardiomyocytes were paced by 5 ms, 1 mW/mm^2 light pulses (blue), delivered at 1 Hz (panel a, 5 pulses shown), 5 Hz (panel b, 10 pulses shown) or 20 Hz (panel c, 10 pulses shown). Note the different time scales. In panels (a–c), row I shows the triggered voltage changes (action potentials); row II shows the $I_{ChR2(Vclamp)}$ in response to the light pulses, if the voltage is clamped at 285 mV; row III shows overlaid, highly similar true $I_{ChR2(AP)}$ (black) and approximated $I_{ChR2(AP)}$ (red) by the proposed method in Figure 3; and row IV shows the error (difference) between the overlaid black and red traces in row III.

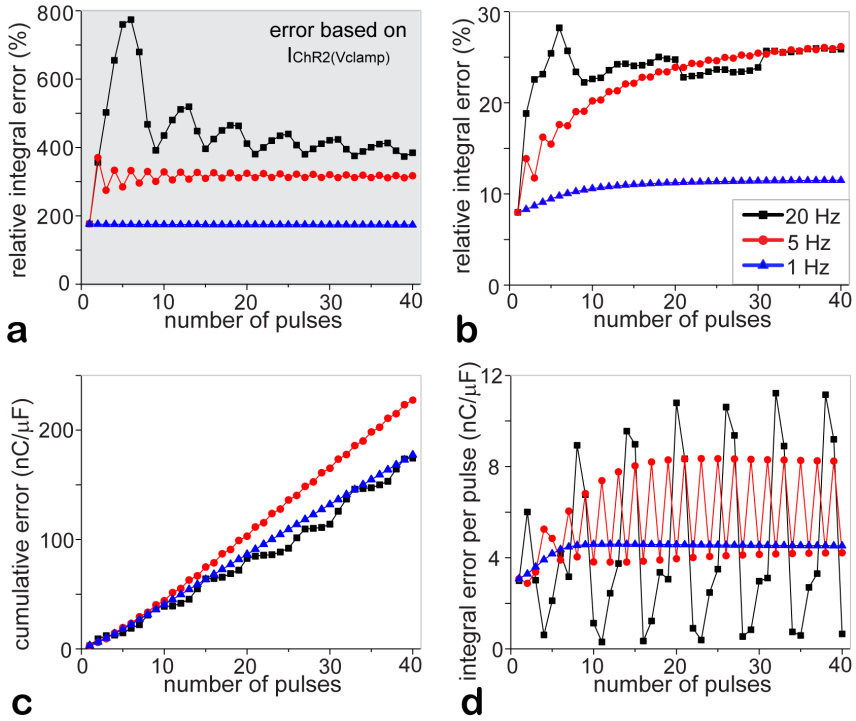

Figure 5 | Summary of error estimates as function of stimulation frequency and pulse number: (a) (shaded). Relative time-integrated error (as % of the time-integrated $I_{ChR2(AP)}$, cumulative over the indicated number of light pulses/beats) if $I_{ChR2(Vclamp)}$ is used to estimate the true $I_{ChR2(AP)}$ (i.e. error between rows II and III in Figure 4a–c). (b–d). Errors if the new (*I–V* curve-based) approximation is used to estimate the true $I_{ChR2(AP)}$ (compare the overlaid traces in rows III of Figure 4a–c, as well as the resultant difference errors displayed in rows IV of Figure 4a–c). (b). Relative time-integrated error (in % of the time-integrated $I_{ChR2(AP)}$); (c). Cumulative absolute time-integrated error (in units of charge nC/µF); (d). Absolute time-integrated error per pacing period (in nC/µF). Light pulses were 5 ms at 1 mW/mm^2, delivered at 1 Hz (blue), 5 Hz (red) or 20 Hz (black), as indicated by example traces in Figure 4. Note that 40 pulses correspond to 40 s, 8 s and 2 s time interval for the three pacing frequencies.

an atrial cell AP, which operates extensively at voltages below 0mV and has a more gradual repolarization, a light pulse delivered during an ongoing AP produces higher magnitude inward $I_{ChR2(AP)}$ and has a better chance at influencing the electrical state of the cell, i.e. altering the action potential shape (Figure 6, right). The two approaches outlined here in Figures 2 and 3 are applicable in uncovering the

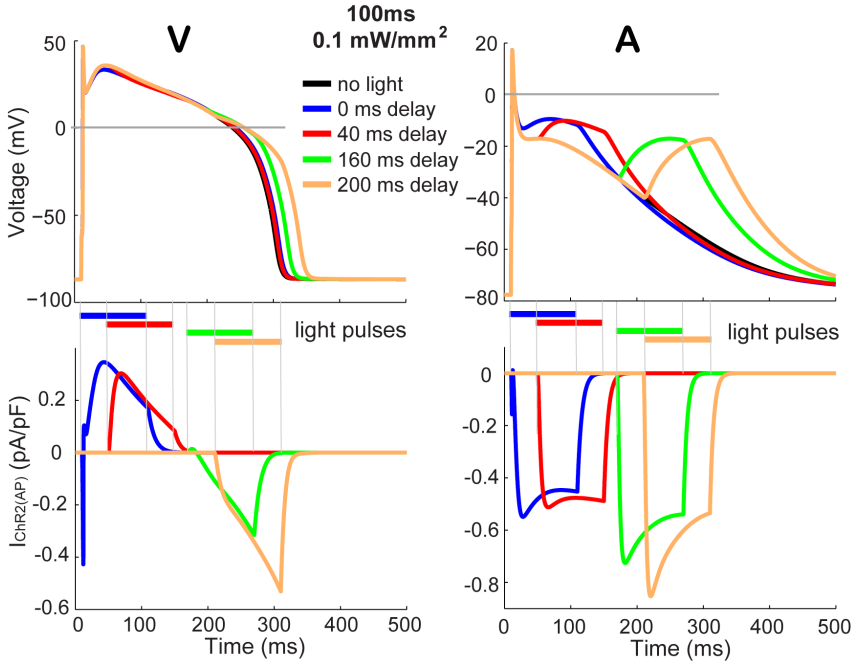

Figure 6 | **Light pulses, applied during an ongoing action potential, trigger distinct $I_{ChR2(AP)}$ in different cardiac cell types due to instant voltage feedback.** Electrically-triggered action potentials in human ventricular cells[8] (V, left) and in atrial cells[23] (A, right), and the effect of a light pulse (470 nm, 100 ms, 0.1 mW/mm^2), applied at variable delay with respect to the electrical stimulus (current injection was 0.5 ms. 50 pA/pF). The respective underlying $I_{ChR2(AP)}$ currents are shown for V and A on the bottom. Timing of the light pulses is indicated by color-coded horizontal bars.

underlying opsin currents (Figure 6, bottom row) during such optical perturbations of ongoing electrical activity in different cell types. Such information can be useful in designing optical cardioversion strategies[20,21] or feedback strategies for suppression of ongoing pathological neural excitations[22].

In summary, using the "*optical APclamp*" or its proposed simple approximation, one can reveal the true nature of the opsin contribution *during* light-triggered action potentials or during optical perturbation of ongoing electrical activity in different cells and appreciate the feedback exerted on the opsin current during membrane voltage changes. These aspects of the ChR2 action are important in better understanding its function in mammalian excitable tissue, including brain and heart, and evaluating differences between optical and electrical stimulation. The approaches discussed here are potentially applicable to other opsins with separable light- and voltage dependencies; they can be used to rationally improve and optimize the performance of engineered opsins for operation in specific cells and tissues.

1. Nagel, G. *et al.* Channelrhodopsin-2, a directly light-gated cation-selective membrane channel. *Proc Natl Acad Sci U S A* **100**, 13940–13945 (2003).
2. Nagel, G. *et al.* Light activation of channelrhodopsin-2 in excitable cells of Caenorhabditis elegans triggers rapid behavioral responses. *Curr Biol* **15**, 2279–2284 (2005).
3. Boyden, E. S., Zhang, F., Bamberg, E., Nagel, G. & Deisseroth, K. Millisecond-timescale, genetically targeted optical control of neural activity. *Nat Neurosci* **8**, 1263–1268 (2005).
4. Zhao, S. *et al.* Cell type-specific channelrhodopsin-2 transgenic mice for optogenetic dissection of neural circuitry function. *Nat Methods* **8**, 745–752 (2011).
5. Arenkiel, B. R. *et al.* In vivo light-induced activation of neural circuitry in transgenic mice expressing channelrhodopsin-2. *Neuron* **54**, 205–218 (2007).
6. Jego, S. *et al.* Optogenetic identification of a rapid eye movement sleep modulatory circuit in the hypothalamus. *Nat Neurosci* **16**, 1637–1643 (2013).
7. Williams, J. C. *et al.* Computational Optogenetics: Empirically-Derived Voltage- and Light-Sensitive Channelrhodopsin-2 Model. *PLoS Comput Biol* **9**, e1003220 (2013).
8. ten Tusscher, K. H. & Panfilov, A. V. Alternans and spiral breakup in a human ventricular tissue model. *Am J Physiol Heart Circ Physiol* **291**, H1088–1100 (2006).
9. Clay, J. R., Paydarfar, D. & Forger, D. B. A simple modification of the Hodgkin and Huxley equations explains type 3 excitability in squid giant axons. *J R Soc Interface* **5**, 1421–1428 (2008).
10. Entcheva, E. Cardiac optogenetics. *Am J Physiol Heart Circ Physiol* **304**, H1179–1191 (2013).
11. Llinas, R., Sugimori, M. & Simon, S. M. Transmission by presynaptic spike-like depolarization in the squid giant synapse. *Proc Natl Acad Sci U S A* **79**, 2415–2419 (1982).
12. Doerr, T., Denger, R., Doerr, A. & Trautwein, W. Ionic currents contributing to the action potential in single ventricular myocytes of the guinea pig studied with action potential clamp. *Pflugers Arch* **416**, 230–237 (1990).
13. Grossman, N. *et al.* The spatial pattern of light determines the kinetics and modulates backpropagation of optogenetic action potentials. *J Comput Neurosci* **34**, 477–488 (2013).
14. Hegemann, P., Ehlenbeck, S. & Gradmann, D. Multiple photocycles of channelrhodopsin. *Biophys J* **89**, 3911–3918 (2005).
15. Nikolic, K. *et al.* Photocycles of channelrhodopsin-2. *Photochem Photobiol* **85**, 400–411 (2009).
16. Gunaydin, L. A. *et al.* Ultrafast optogenetic control. *Nat Neurosci* **13**, 387–392 (2010).
17. Berndt, A. *et al.* High-efficiency channelrhodopsins for fast neuronal stimulation at low light levels. *Proc Natl Acad Sci U S A* **108**, 7595–7600 (2011).
18. Kleinlogel, S. *et al.* Ultra light-sensitive and fast neuronal activation with the Ca(2)+-permeable channelrhodopsin CatCh. *Nat Neurosci* **14**, 513–518 (2011).
19. Beppu, K. *et al.* Optogenetic countering of glial acidosis suppresses glial glutamate release and ischemic brain damage. *Neuron* **81**, 314–320 (2014).
20. Boyle, P. M., Williams, J. C., Ambrosi, C. M., Entcheva, E. & Trayanova, N. A. A comprehensive multiscale framework for simulating optogenetics in the heart. *Nat Commun* **4**, 2370 (2013).
21. Ambrosi, C. M. & Entcheva, E. Optogenetics' promise: pacing and cardioversion by light? *Future Cardiol* **10**, 1–4 (2014).
22. Krook-Magnuson, E., Armstrong, C., Oijala, M. & Soltesz, I. On-demand optogenetic control of spontaneous seizures in temporal lobe epilepsy. *Nat Commun* **4**, 1376 (2013).
23. Courtemanche, M., Ramirez, R. J. & Nattel, S. Ionic mechanisms underlying human atrial action potential properties: insights from a mathematical model. *Am J Physiol* **275**, 301–321 (1998).

Acknowledgments

This work is supported by NIH-NHLBI grant to E.E., R01 HL-111649. We thank Sriharsha Tikkireddy for help generating some of the data.

Author contributions

E.E. and J.C.W. wrote the manuscript text and prepared the figures. Both authors reviewed the manuscript.

Additional information

Competing financial interests: The authors declare no competing financial interests.

How to cite this article: Entcheva, E. & Williams, J.C. Channelrhodopsin2 Current During the Action Potential: "Optical AP Clamp" and Approximation. *Sci. Rep.* **4**, 5838; DOI:10.1038/srep05838 (2014).